JOURNAL OF MATERIALS SCIENCE 17 (1982) 3499–3509

Complex moduli of aligned discontinuous fibre-reinforced polymer composites

R. F. GIBSON
Department of Mechanical Engineering, University of Idaho, Moscow, Idaho 83843, USA
S. K. CHATURVEDI, C. T. SUN
Center for Studies of Advanced Structural Composites, Department of Engineering Sciences, University of Florida, Gainesville, Florida 32611, USA

This paper describes recent analytical and experimental efforts to determine the effects of fibre aspect ratio, fibre spacing, and the viscoelastic properties of constituent materials on the damping and stiffness of aligned discontinuous fibre-reinforced polymer matrix composites. This includes the analysis of trade-offs between damping and stiffness as the above parameters are varied. Two different analytical models show that there is an optimum fibre aspect ratio for maximum damping, and that the predicted optimum aspect ratios lie in the range of actual aspect ratios for whiskers and microfibres when the fibre damping is small. When the fibre damping is great enough, however, the optimum fibre aspect ratio corresponds to continuous fibre reinforcement. Experimental data for E-glass/epoxy specimens are presented for comparison with predictions.

Nomenclature

A_c, A_f, A_m	Cross-sectional area of composite, fibre, and matrix, respectively.
d	Fibre diameter.
E_c^*, E_f^*, E_m^*	Complex extensional modulus of composite, fibre, and matrix, respectively.
E_c', E_f', E_m'	Extensional storage modulus of composite, fibre, and matrix, respectively.
E_c'', E_f'', E_m''	Extensional loss modulus of composite, fibre, and matrix, respectively.
G_m^*	Complex shear modulus of matrix.
G_m'	Shear storage modulus of matrix.
i	$-1^{1/2}$.
K	Defined in Equation A9.
K_1	Defined in Equation A5.
l	Fibre length.
r	Radial distance from centre of fibre.
r_0	Fibre radius.
R	Radius of representative volume element, or one-half of centre-to-centre fibre spacing.
v_f, v_m	Volume fraction of fibre and matrix, respectively.
W_c	Total strain energy stored in a unit volume of composite.
W_f	Strain energy stored in volume v_f of fibre.
W_m	Strain energy stored in a volume v_m of matrix.
$W_{\gamma m}$	Shear strain energy stored in a volume v_m of matrix.
$W_{\epsilon m}$	Extensional strain energy stored in a volume v_m of matrix.
w_{rm}	Shear strain energy stored in the matrix in $r_0 \leqslant r \leqslant R$.
w_f	Extensional strain energy stored in a single fibre.
x	Distance along fibre from end of fibre.
α	Defined in Equation 12.
β	Defined in Equation 2.
β^*	Defined in Equation A2.
ϵ	Extensional (longitudinal) strain.
η_c, η_f, η_m	Extensional loss factor of composite, fibre, and matrix, respectively.
η_{Gm}	Shear loss factor of matrix.
θ	Polar angle measured in a plane perpendicular to fibre axis.
$\bar{\sigma}_c, \bar{\sigma}_f, \bar{\sigma}_m$	Average longitudinal stress in com-

0022–2461/82/123499–11$03.82/0

posite, fibre, and matrix, respectively.
σ_f Longitudinal stress in fibre.
τ Shear stress in matrix.
ψ Defined in Equation 27.

1. Introduction

It is a well-known fact that light-weight fibre-reinforced plastic materials have excellent strength and stiffness, and much effort has been devoted to the improvement and optimization of these properties in various structures. Many applications of these materials require good vibration damping properties as well (e.g. aerospace structures, helicopter rotor blades, circuit boards, high-speed printer components). Due in part to extensive accumulated experience with conventional structural metals having poor internal damping characteristics, the potential for significant improvement and optimization of damping in advanced fibre-reinforced plastics has not been fully realized, however. At the same time, discontinuous fibre reinforcement has not been emphasized in advanced composite materials research because of the higher strengths and stiffnesses currently available in continuous fibre composites. However, the results presented in this paper indicate that the vibration damping properties of polymer matrix, fibre-reinforced composite materials may be significantly improved and possibly optimized by using discontinuous fibres rather than continuous fibres. More specifically, this paper describes recent efforts to determine the effects of fibre aspect ratio, fibre spacing, and the viscoelastic properties of matrix and fibre materials on the damping and stiffness of aligned discontinuous fibre-reinforced polymer matrix composite materials. The analysis of trade-offs between damping and stiffness is also included.

The damping properties of continuous fibre composites have been studied by a number of investigators, as shown in several previous review papers [1–4]. There are relatively few reports of such work on discontinuous fibre composites, however. Studies reported by McLean and Read [5] and Gibson and Yau [6] indicate that the damping in a given composite can be improved by using discontinuous fibres rather than continuous fibres. One possible explanation for this phenomenon is the presence of shear stress concentrations at the numerous fibre ends in a discontinuous fibre composite and the resulting shear stress transfer to the viscoelastic matrix. It is known that shear deformation causes most of the vibrational energy dissipation in viscoelastic materials such as polymers [7]. A previous analysis of discontinuous constrained viscoelastic layer damping by Plunkett and Lee [7] appears to offer an analogous solution for the case of discontinuous aligned fibre reinforcement. This analogy, which was also observed by Bert [4], is based on the similarities of the interfacial shear stress distributions along discontinuous constraining layers and along discontinuous reinforcing fibres. The approximate stress distribution along a discontinuous fibre embedded in a matrix material was first reported by Cox [8]. The analytical and experimental work by Plunkett and Lee [7] showed that there is an optimum constraining layer aspect ratio for maximum damping in the constrained viscoelastic layer. Thus, the existence of such an optimum aspect ratio for the short-fibre composite seems apparent. The optimum aspect ratio for damping is not necessarily the best for stiffness, however. So it is important to study the influence of the various governing parameters on both damping and stiffness.

In the present work, two approaches to the solution for the complex modulus of a discontinuous aligned fibre composite were based on the Cox stress distribution. In the energy approach, the energy stored in the fibre and matrix and the energy dissipated due to interfacial shear stresses were calculated, and the energy balance on the representative volume element provided the values of storage as well as loss moduli. The other approach involved the derivation of the expression for the elastic stiffness of the discontinuous composite based upon the average fibre stress and the force balance between fibre and matrix. The elastic–viscoelastic correspondence principle was then used to obtain the expression for the complex modulus. Both approaches verified the existence of a theoretically optimum fibre aspect ratio, as seen later.

Preliminary experimental data on damping and stiffness of discontinuous aligned composites was obtained by using a resonant dwell, forced flexural vibration technique to test E-glass/epoxy specimens having several fibre aspect ratios. Analytical and experimental results are compared and discussed and conclusions regarding future directions of this research are presented.

2. Analysis

There appear to be two primary sources of enhanced damping or energy dissipation in fibre-reinforced polymeric matrix materials; (1) the viscoelastic behaviour of the bulk matrix and the interface, and (2) the friction at the interface caused by relative motion between matrix and fibre. Both of these effects may be significant in discontinuous fibre composites in which high shear stresses are developed at the fibre–matrix interface. When a short-fibre composite is subjected to a cyclic strain, the matrix at the fibre interface near the ends of the fibre undergoes a high cyclic shear strain, thus producing significant viscoelastic energy loss. It should be noted that most of the energy dissipation in polymers is due to shear strains, and very little is caused by dilatational strains. Thus, even the unreinforced resin would dissipate energy under most loading situations. Only in pure hydrostatic loading would there be no energy dissipation.

The shear stress concentration may also induce plastic effects as well as partial debonding at the fibre–matrix interface that would result in slip between fibre and matrix and corresponding frictional losses. Such a fibre–matrix debonding would, however, effect adversely the strength and stiffness of the composite. Therefore, it is desirable to have a strong interfacial bond such that slip at the interface can be avoided. Thus, the most viable mechanism of enhanced dissipation appears to be the shear deformation in the matrix caused by shear stress concentration near the fibre ends.

Looking towards the stress transfer mechanism between fibre and the matrix, various theories tend to agree that there are several parameters (e.g. fibre aspect ratio (length/diameter), fibre volume fraction (v_f), fibre/matrix modulus ratio (E'_f/E'_m) etc.) that influence the shear stress distribution at the interface. The matrix surrounding a short fibre in a composite experiences a three-dimensional state of stress even though the composite may only be subjected to a uniaxial state of stress. The situation becomes further complicated when the interaction with neighbouring fibres is also taken into account. We therefore chose to use a "mechanics of materials" approach that could reasonably predict the stress transfer at the interface. The shear lag analysis due to Cox [8] appeared to be reasonable for this purpose. This theory is based upon the assumptions that there is a perfect bond between the fibre and the matrix, that both matrix and fibre are linearly elastic, and that the representative volume element is subjected to a uniform extensional strain along the fibre direction. According to this theory, the shear stress in the matrix at a distance x along the fibre and a radius r (Fig. 1) is given by the equation:

$$\tau = \frac{r_0^2 E'_f \epsilon \beta}{2r} \frac{\sinh[\beta(l/2 - x)]}{\cosh(\beta l/2)}, \quad (1)$$

where

$$\beta^2 = \frac{G'_m}{E'_f} \frac{2}{r_0^2 \ln(R/r_0)}. \quad (2)$$

Other approximate analyses by Dow [9], Rosen [10], and Kelly and Tyson [11] appear to give very similar results to that of Cox and differ only in the values of β. In all the analyses β is proportional to $(E'_m/E'_f)^{1/2}$ and differences occur only in the term involving the volume fraction of fibres; ($\ln R/r_0$ in Equation 2). In spite of the shortcomings, Equation 1 is a good approximation to that obtained by a much more sophisticated analysis by Smith and Spencer [12]. It is realized, however, that all of these analyses are based upon a single fibre model and ignore the effect of neighbouring fibres, of fibre end conditions and of abutting fibre ends. Some of the geometrical parameters, however, are shown to have opposing effects on the shear stress concentration.

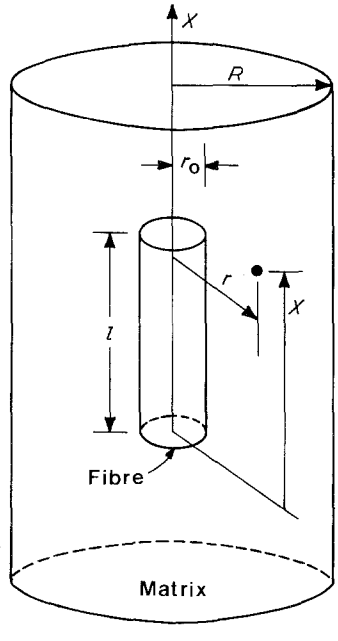

Figure 1 Representative volume element.

On one hand, the photoelastic study of a single fibre embedded in a matrix by Tyson and Davies [13] shows that the shear stress near the fibre end is considerably larger than that predicted by Equation 1. On the other hand, the experimental and analytical studies by Carrara and McGarry [14], MacLaughlin [15], Iremonger and Wood [16], and Barker and MacLaughlin [17] showed that by decreasing the centre-to-centre fibre spacing (increasing v_f) the interfacial shear stress is reduced. It was also found that by decreasing the spacing between abutting fibre ends, the interfacial shear stress along the fibre was reduced. There may also be residual shear stresses at the fibre discontinuities, however, their nature and effects are not well known. Thus, it is well established that the stresses in a discontinuous composite are highly complex and it does not seem possible to take into account all the parameters that influence the stress in a closed-form solution.

In spite of such complexities, Cox's model appears to predict reasonably well the interfacial shear stress distribution. McLean and Read [5] used this model to estimate damping in rubber-like material unidirectionally reinforced with discontinuous fibres. As shown later, however, their expressions are not complete because damping for the unreinforced composite (i.e., $v_f = 0$) and for continuous reinforcement (i.e. large fibre aspect ratios) cannot be deduced from them.

Two approaches to the solution for complex modulus that can be adopted from Cox's stress distribution are discussed in the paragraphs to follow.

2.1. Energy approach

In this approach, the energy stored in the fibre and matrix and the energy dissipated due to interfacial shear stresses are used to find the values of storage as well as loss moduli. The analysis was carried out under the following assumptions: (a) the fibre is linearly elastic; (b) the matrix is a linearly viscoelastic; (c) there is a perfect bond between the fibre and the matrix and the interface has the same viscoelastic properties as that of the bulk matrix.

The above assumptions implicitly state that the strain energy is stored in both the constituent materials but that dissipation of energy takes place only in the matrix. Furthermore, it should be noted that the matrix between fibres undergoes shear deformation due to the presence of short fibres in addition to the deformation equivalent to the applied composite strain.

If the longitudinal strain in the composite, the fibre and the matrix can be assumed to be ϵ, the shear strain energy stored in a cylinder of matrix of radius R surrounding each fibre is given by:

$$w_{rm} = \int_{r_0}^{R} \int_{0}^{l/2} \int_{0}^{2\pi} \frac{\tau^2}{G'_m} r \, dr \, dx \, d\theta, \qquad (3)$$

where the shear stress τ is given by Equation 1. The total shear strain energy, $W_{\gamma m}$, stored in the volume, v_m, of matrix in a unit volume of composite is

$$W_{\gamma m} = \frac{w_{rm} v_m}{\pi(R^2 - r_0^2) l} \qquad (4a)$$

or

$$W_{\gamma m} = \frac{\epsilon^2 v_m E'_f}{4[(R^2/r_0^2) - 1]} \left(\frac{\tanh \beta l/2}{\beta l/2} - \frac{1}{\cosh^2 \beta l/2} \right). \qquad (4b)$$

The additional strain energy in the volume v_m of matrix due to composite extensional strain, ϵ, is

$$W_{\epsilon m} = \tfrac{1}{2} \epsilon^2 E'_m v_m. \qquad (5)$$

This part of stored energy in the matrix was not considered by McLean and Read [5]. The strain energy in the fibres can also be calculated using longitudinal fibre stress due to Cox [8] as:

$$\sigma_f = \epsilon E'_f \left\{ 1 - \frac{\cosh[\beta(l/2 - x)]}{\cosh \beta l/2} \right\}. \qquad (6)$$

The strain energy stored in a single fibre is

$$w_f = \int_0^{l/2} \frac{\pi r_0^2 \sigma_f^2}{E'_f} \, dx. \qquad (7)$$

Therefore, the strain energy, W_f, in volume, v_f, of fibres contained in a unit volume of composite can be calculated from

$$W_f = \frac{v_f w_f}{\pi r_0^2 l}. \qquad (8)$$

The storage modulus, E'_c, of the composite can be obtained as

$$E'_c = \frac{2W_c}{\epsilon^2} = \frac{2(W_m + W_f)}{\epsilon^2}, \qquad (9)$$

where

$$W_m = W_{\gamma m} + W_{\epsilon m}. \qquad (10)$$

Combining Equations 4b, 5, 8, 9 and 10, it is seen that

$$\frac{E'_C}{E'_m} = \frac{E'_f}{E'_m} v_f + v_m + \frac{E'_f}{E'_m}\left\{\frac{v_f}{\beta l} - \frac{v_m}{\beta l[(R^2/r_0^2)-1]}\right\} \times \left[\frac{\alpha \sinh(\beta l) + \beta l}{1 + \cosh \beta l}\right] \quad (11)$$

where

$$\alpha = \frac{1 - v_f[(3R^2/r_0^2) - 2]}{v_f(R^2/r_0^2) - 1}. \quad (12)$$

As we assumed that the fibres do not contribute significantly to the dissipation of energy, the composite loss modulus, E''_c, can be given as

$$\frac{E''_c}{E'_c} = \eta_c = \frac{\eta_m W_m}{W_c}, \quad \text{or} \quad E''_c = \frac{2E''_m W_m}{E'_m \epsilon^2}. \quad (13)$$

Substituting Equations 4b, 5 and 10 into Equation 13, we get

$$\frac{E''_c}{E''_m} = v_m \left\{\frac{E'_f}{E'_m} \cdot \frac{1}{2[(R^2/r_0^2)-1]} \times \left(\frac{\tanh \beta l/2}{\beta l/2} - \frac{1}{\cosh^2 \beta l/2}\right) + 1\right\}. \quad (14)$$

For practical calculations the ratio R/r_0 in Equations 11, 12 and 14 may be expressed in terms of the fibre volume fraction as shown in the Appendix.

2.2. Force-balance approach

In this approach, the expression for the elastic stiffness of the discontinuous composite is derived from the average fibre stress based upon Cox's fibre-stress distribution. Then the elastic–viscoelastic correspondence principle [18] is used to obtain the expression for the complex modulus. This involves the replacement of the elastic moduli of composite, fibre and matrix in all expressions with the corresponding viscoelastic complex moduli for sinusoidal vibration. The complex equation for the composite modulus then becomes two real equations for storage and loss moduli.

All the earlier assumptions stand except that the fibre can now contribute to energy dissipation and therefore the loss factor, η_f, may be nonzero.

Based on the fibre-stress distribution (Equation 6) the average fibre stress can be written as

$$\bar{\sigma}_f = \frac{1}{l/2}\int_0^{l/2} \sigma_f \, dx = \epsilon E'_f \left[1 - \frac{\tanh(\beta l/2)}{\beta l/2}\right]. \quad (15)$$

For static equilibrium, the total longitudinal force applied to the composite must be

$$P = \bar{\sigma}_c A_c = \bar{\sigma}_f A_f + \bar{\sigma}_m A_m, \quad (16)$$

therefore

$$\sigma_c = E'_c \epsilon = \bar{\sigma}_f v_f + \bar{\sigma}_m v_m. \quad (17)$$

Since the composite, the fibre, and the matrix all have the same extensional strain, ϵ, Equation 17 reduces to

$$E'_c = E'_f \left(1 - \frac{\tanh \beta l/2}{\beta l/2}\right) v_f + E'_m v_m. \quad (18)$$

Then according to elastic–viscoelastic correspondence principle, Equation 18 can be written as

$$E^*_c = E^*_f \left(1 - \frac{\tanh \beta^* l/2}{\beta^* l/2}\right) v_f + E^*_m v_m, \quad (19)$$

or

$$E'_c + iE''_c = (E'_f + iE''_f)v_f \left(1 - \frac{\tanh \beta^* l/2}{\beta^* l/2}\right) + (E'_m + iE''_m)v_m. \quad (20)$$

The above equation can be simplified to obtain storage and loss moduli of the discontinuous composite by separating the real and imaginary parts and by neglecting higher order terms in the loss factors. The results are (see Appendix).

$$E'_c = E'_f v_f \left(1 - \frac{\tanh \beta l/2}{\beta l/2}\right) - \frac{E''_f v_f}{2}(\eta_{Gm} - \eta_f) \times \left(\frac{\tanh \beta l/2}{\beta l/2} - \frac{1}{\cosh^2 \beta l/2}\right) + E'_m v_m, \quad (21)$$

$$E''_c = E''_f v_f \left(1 - \frac{\tanh \beta l/2}{\beta l/2}\right) + \frac{E'_f v_f}{2}(\eta_{Gm} - \eta_f) \times \left(\frac{\tanh \beta l/2}{\beta l/2} - \frac{1}{\cosh^2 \beta l/2}\right) + E''_m v_m. \quad (22)$$

A number of special cases can be derived from these general equations. For continuous reinforcement, the fibre aspect ratio, l/d, is very large, and the storage and loss moduli take the familiar forms

$$E'_c = E'_f v_f + E'_m v_m, \quad (23)$$

and

$$E''_c = E''_f v_f + E''_m v_m. \quad (24)$$

If we assume that $\eta_f = 0$, which means that the fibres are non-dissipative, then Equations 21 and 22 for a discontinuous composite will reduce to:

$$\frac{E'_c}{E'_m} = \frac{E'_f}{E'_m} v_f \left[1 - \frac{\tanh \beta l/2}{\beta l/2}\right] + v_m, \quad (25)$$

and

$$\frac{E''_c}{E''_m} = \frac{E'_f}{E''_m} v_f \frac{\eta_{Gm}}{2} \left(\frac{\tanh \beta l/2}{\beta l/2} - \frac{1}{\cosh^2 \beta l/2}\right) + v_m \ . \quad (26)$$

Equation 26 is similar to Equation 14, which was derived using an energy approach.

From the expressions for the loss modulus and the equations in the Appendix, it becomes apparent that

$$\frac{E''_c}{E''_m} = \psi(E'_f/E'_m, v_f, l/d, \eta_f, \eta_{Gm}, \text{packing geometry}). \quad (27)$$

The influence of these independent parameters on the loss modulus can then be investigated. The fibre aspect ratio, l/d, turns out to have the most interesting effect. The optimum value of the loss modulus from Equation 22 can be found from the condition

$$\frac{\partial E''_c}{\partial (l/d)} = 0, \quad (28)$$

which leads to the equation

$$\frac{2 \cosh^2 (\beta l/2)}{\beta^2 l^2} \frac{1}{\beta l \cdot \tanh (\beta l/2)} = \frac{\eta_{Gm} - \eta_f}{\eta_{Gm} - 3\eta_f}. \quad (29)$$

It is very interesting to note that Equation 29 will have different solutions depending upon the relative values of the loss factors η_{Gm} and η_f. It is instructive to first discuss some special cases of this equation.

If we assume that $\eta_f = 0$, then Equation 29 can be simplified to

$$\tanh \frac{\beta l}{2} = \frac{\sinh \beta l}{\beta^2 l^2} - \frac{1}{\beta l}. \quad (30)$$

This equation can also be derived from Equations 14 or 26 by using the condition in Equation 28. This equation has the unique solution $\beta l = 3.28$. That is, when the fibres contribute no damping, maximum damping in the composite occurs for

$$\left(\frac{l}{d}\right)_{opt} = 3.28K, \quad (31)$$

where K is a function of E'_f, E'_m, v_f and fibre packing geometry (see Appendix). It is interesting to note that this is the same aspect ratio as that reported by Plunkett and Lee [7] for constrained layer damping. Although the two approaches predict the same optimum l/d, the predicted loss moduli may differ from each other. The difference is due to the fact that the energy approach takes into account the actual (Cox) shear stress distribution, while the force-balance approach only uses the average stresses.

The condition $\eta_f \geqslant \eta_{Gm}/3$ in Equation 29 leads to maximum damping for $\beta l = \infty$, which means that large fibre aspect ratio (i.e. continuous fibre reinforcement) will provide maximum damping when the fibre damping is great enough. Thus, when $\eta_f < \eta_{Gm}/3$, $(l/d)_{opt} = 3.28K$, and when $\eta_f \geqslant \eta_{Gm}/3$, $(l/d)_{opt} = \infty$. Graphical results from both analytical approaches will be presented and discussed later in this paper, along with experimental results.

3. Experiments

Preliminary experimental data on damping and stiffness of discontinuous-aligned fibre composites was obtained by using a resonant dwell, forced flexural vibration technique [19] to test E-glass/epoxy specimens having four different fibre aspect ratios. The experimental technique is described by Gibson *et al.* [19] except for one detail. Since the materials tested in [19] had relatively high matrix volume fractions, the damping was much higher than the damping in the materials being discussed here. Thus, the parasitic losses in the apparatus were more likely to cause errors in the current measurements. As a result, it was necessary to use epoxy shoulders on the specimens, as described by Gibson and Plunkett [20]. The purpose of these shoulders was to shift the clamping surface away from the region of high strain on the surface of the specimen, thus reducing parasitic frictional losses in this area to an acceptable level.

Specimens were fabricated by cutting 3M Scotchply 1003 pre-preg tape into strips of length l and placing these strips end-to-end in a staggered 15 ply lay-up sequence before final autoclave curing (Fig. 2). Four types of specimens, each with different fibre length, were fabricated. Fibre lengths were 6.35 mm (0.25 in.), 12.7 mm (0.5 in.), 25.4 mm (1.0 in.), and 254 mm (10 in.), and three specimens of each fibre length were tested to get

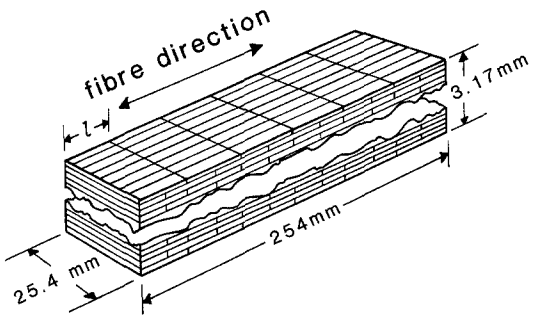

Figure 2 Specimen configuration.

average values of damping and stiffness. Fibre volume fractions, as determined from resin burn-out tests, were typically near $v_f = 0.5$. Test temperatures were $24 \pm 1^\circ$ C, relative humidity was $48 \pm 2\%$, and test frequencies ranged from 140 to 162 Hz. These frequencies corresponded to the fundamental flexural modes of each specimen. Testing was done in air at sufficiently low amplitudes so that air damping was not significant.

Each experiment yielded values of E'_c and η_c [19, 20], then E''_c was calculated from $E''_c = \eta_c E'_c$. Since the properties presumably did not vary through the thickness of the specimen, the measured flexural modulus was assumed to be the same as the extensional modulus. This would not be true if the ply properties varied through the thickness, or if off-axis shear coupling effects came into play. Values of E'_m, η_m, E''_m and E'_f were taken from Gibson and Plunkett [20], since the same materials were used in these earlier experiments. The matrix shear loss factor, η_{Gm}, was found from η_m, the static properties of the matrix, and the viscoelastic forms of the relationships between isotropic elastic constants, under the assumption that the matrix is viscoelastic in shear but elastic in dilatation [20]. Data on the fibre loss factor, η_f, was not available, but estimates can be made as shown in the next section.

4. Discussion and conclusions

In Fig. 3, the predicted (Equations 14 and 26) and measured complex moduli for E-glass/epoxy are plotted against the fibre aspect ratio. Composite moduli are normalized to the matrix moduli for comparison. The differences in the results for the two models are due to the fact that the energy model is based on the Cox fibre stress distribution, while the force-balance model uses the average of this stress distribution. Fig. 3 shows that both analytical models predict an optimum fibre aspect ratio, l/d, for maximum damping. The optimum l/d for damping is less than the minimum aspect ratio required for maximum stiffness, however. The curves in Fig. 3 were generated by assuming

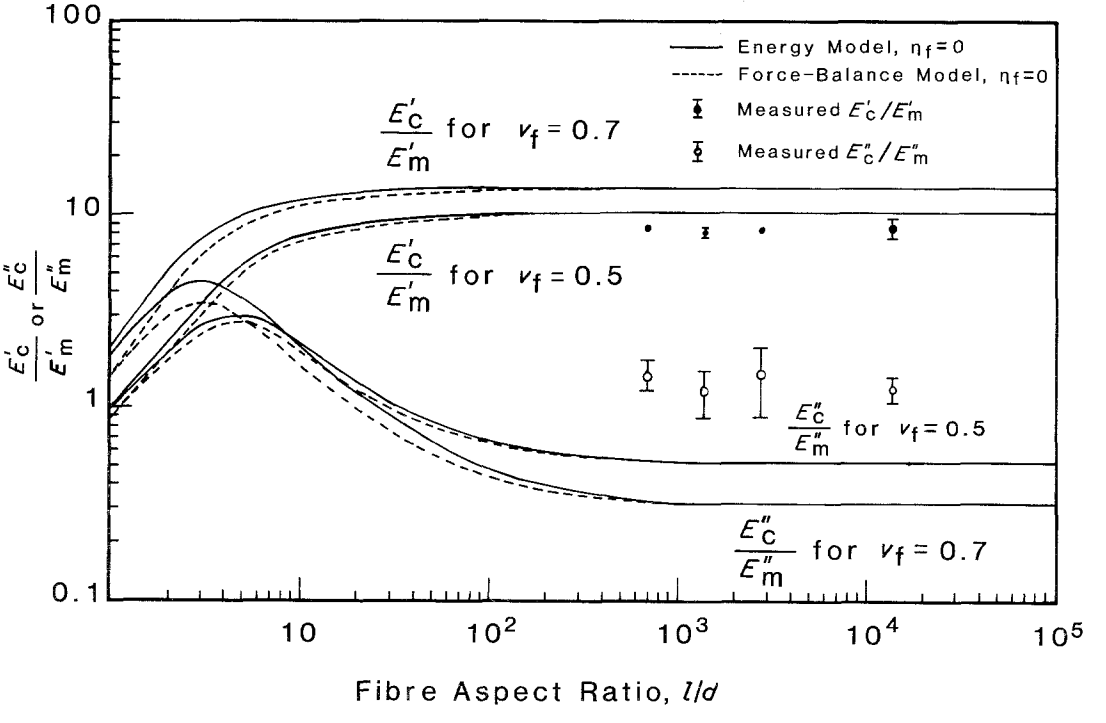

Figure 3 Measured and predicted complex moduli for E-glass/epoxy.

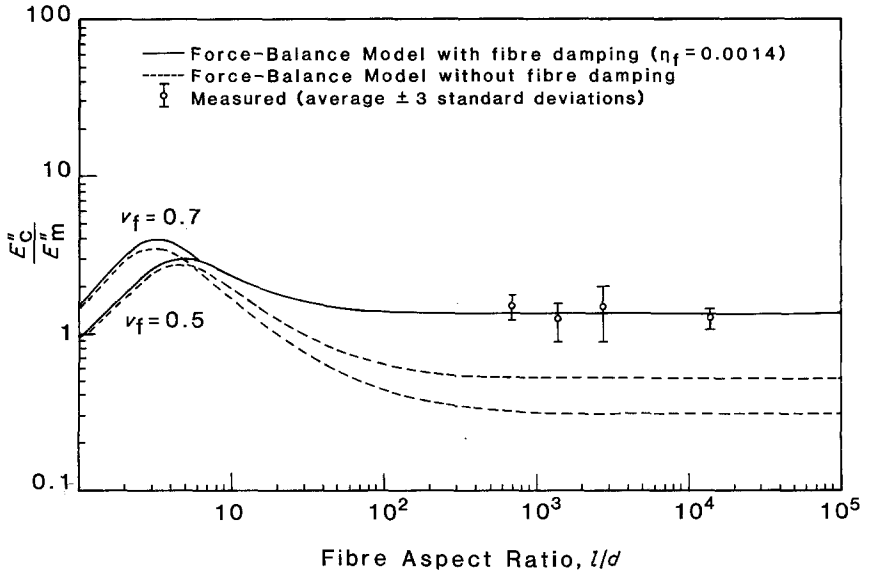

Figure 4 Assumed fibre loss factor gives better agreement with experimental damping data.

that all energy dissipation occurs in the matrix. Better agreement with measured loss moduli is obtained by assuming a reasonable fibre loss factor, however, as shown in Fig. 4 (Equations 22 and 26). The general behaviour of the loss modulus with regard to aspect ratio curves with increased fibre damping is shown clearly in Fig. 5. Thus, when $\eta_f < \eta_{Gm}/3$ (which appears to be the case for most common reinforcing fibres), maximum damping in the composite is predicted for very low aspect ratios. When $\eta_f \geqslant \eta_{Gm}/3$, however, continuous fibre reinforcement gives the best composite damping characteristics. The trends observed in Fig. 5 also show the potential advantages of high damping in such fibres as Kevlar [21]. The assumption of either hexagonal or square-packing geometry has little effect on the magnitude of damping or the optimum aspect ratio, as shown in Fig. 6.

During the initial stages of the experiments, it

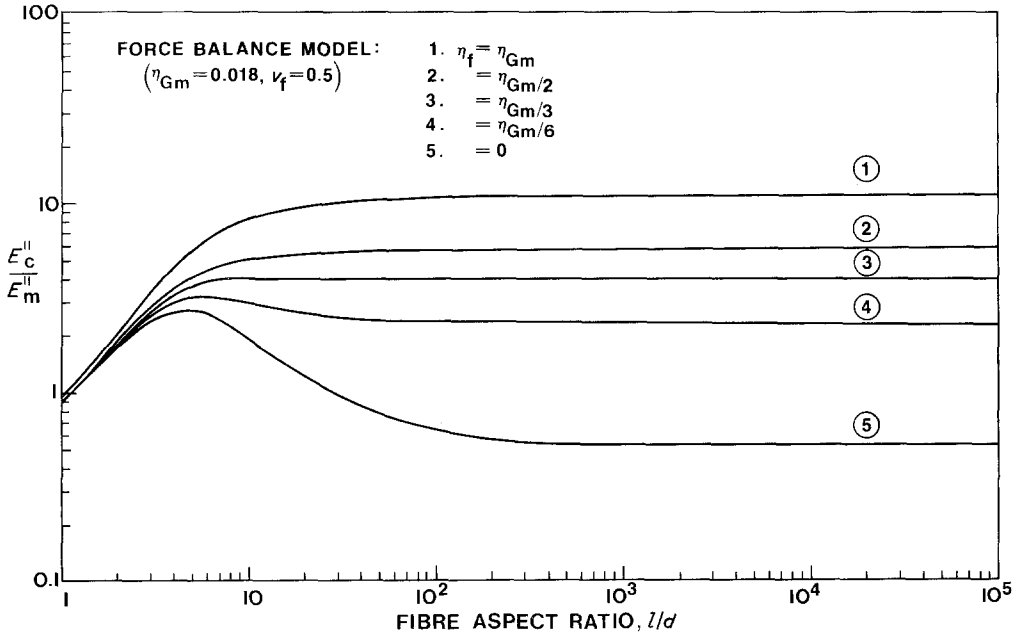

Figure 5 Effect of fibre loss factor on loss modulus of E-glass/epoxy.

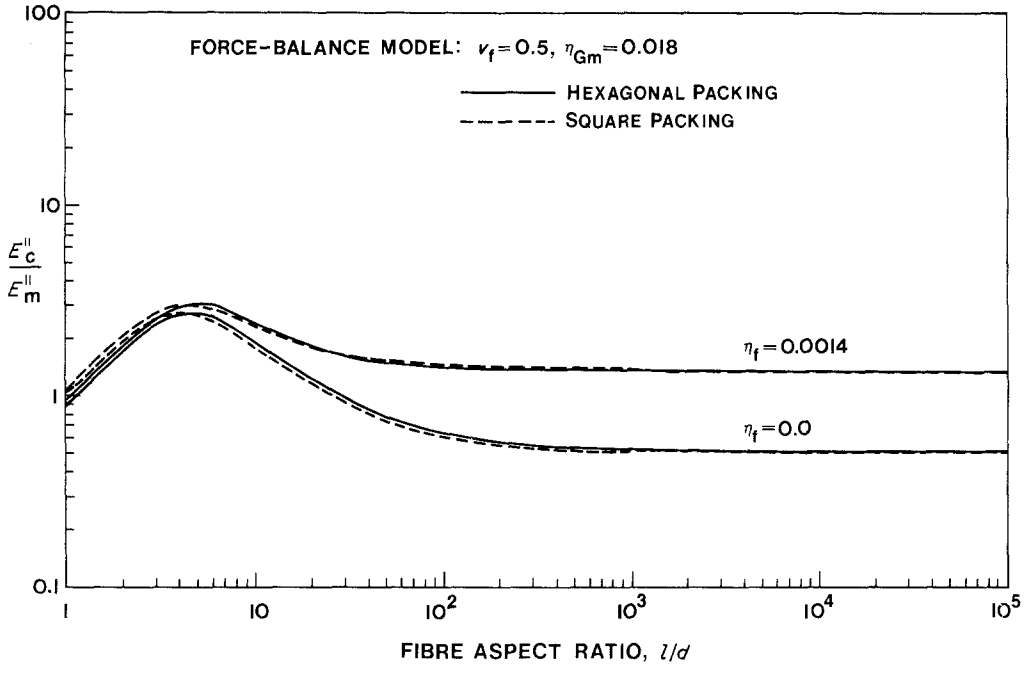

Figure 6 Effect of fibre packing geometry on loss modulus of E-glass/epoxy.

was believed that the actual fibre aspect ratio could be based on the fibre bundle, which contains approximately 1000 fibres. This would have meant that the aspect ratios for the specimens tested would have been much smaller and closer to the optimum values, which was desirable. As the experiments progressed, however, it became apparent that the actual fibre aspect ratio should be based on a single fibre, as plotted in Figs. 3 and 4. Thus, the measured stiffness and damping values turned out to be in a region where the aspect ratio is not important (i.e. continuous fibres). The scatter in the data is thought to be due primarily to small differences in fibre volume fractions for the different specimens. The lowest specimen aspect ratio shown in Figs 3 and 4 corresponds to 6.35 mm (0.25 in.) long strips of prepreg tape, and a fibre diameter of 0.010 mm (0.0004 in.). This is believed to be close to the lower limit of aspect ratios which we can produce by manually cutting the pre-preg tape. As a result of these experiments and additional analytical results to be discussed in the remainder of this paper, we have now shifted our attention to higher modulus fibres.

The analytical models predict that the peak damping values and the optimum aspect ratios are both increased significantly when higher modulus fibres are used, as shown in Fig. 7. These results seem to indicate that near-optimum damping may be achievable in a whisker or micro-fibre composite [22], since the actual aspect ratios for these materials are near the predicted optimum values. Some sacrifice in stiffness is necessary in order to achieve maximum damping, as shown in Fig. 8. In practical short-fibre composites, the fibres are often randomly oriented and there is reason to believe that the shear stress/damping effect is magnified still further by this off-axis fibre orientation [6, 23]. As previously shown in Fig. 5, the potential for still greater improvement exists with polymeric fibres (e.g. Kevlar), which appear to have much higher damping than glass or graphite [21]. Finally, hybrid combinations of continuous fibres for strength and stiffness and short fibres for damping (or mixed fibre types) would appear to offer unlimited design flexibility. The authors are presently planning a systematic analytical and experimental investigation of all of these potential improvements.

The nearly isotropic behaviour and enhanced damping of random short fibre composites are distinct advantages when compared with the highly anisotropic behaviour and relatively low damping in continuous fibre composites. Major improvements in short fibre and hybrid composite materials fabrication techniques and resulting material cost reductions are now taking place

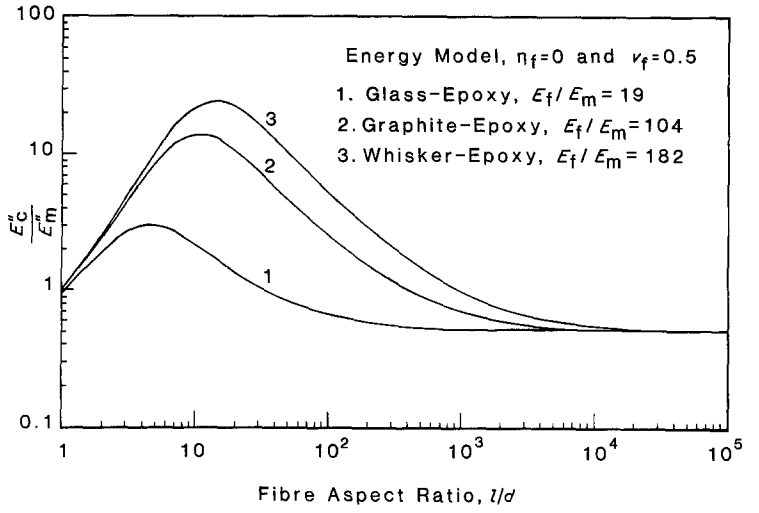

Figure 7 Effect of fibre stiffness on loss modulus of discontinuous aligned composites.

primarily because of high-volume use of these materials in the automobile industry [24]. In addition, the almost certain future availability of higher modulus, higher strength, short fibres and whiskers may mean that short-fibre composites can be used in many applications which presently require continuous fibre reinforcement [22]. Thus, it would appear that these current and anticipated developments make such a damping research programme even more relevant to the continued advancement of structural materials and structural dynamics technology.

Acknowledgements

The authors gratefully acknowledge the financial support for the Center for Studies of Advanced Structural Composites at the University of Florida. We are also indebted to Mr J. D. McMillan of the Department of Engineering Sciences for his excellent work on fabrication of specimens and experimental apparatus. This work was done while Dr Gibson was a visiting Associate Professor at the University of Florida during academic year 1980–1981.

Appendix

The complex modulus for the composite according to the force-balance model was found to be

$$E'_c + iE''_c = (E'_f + iE''_f)v_f\left(1 - \frac{\tanh \beta^* l/2}{\beta^* l/2}\right) + (E'_m + iE''_m)v_m, \quad \text{(A1)}$$

where

$$\beta^* = \left[\frac{G^*_m}{E^*_f}\frac{2}{r_0^2 \ln(R/r_0)}\right]^{1/2}, \quad \text{(A2)}$$

is found by applying the correspondence principle to Equation 2. The ratio R/r_0 in equations such as

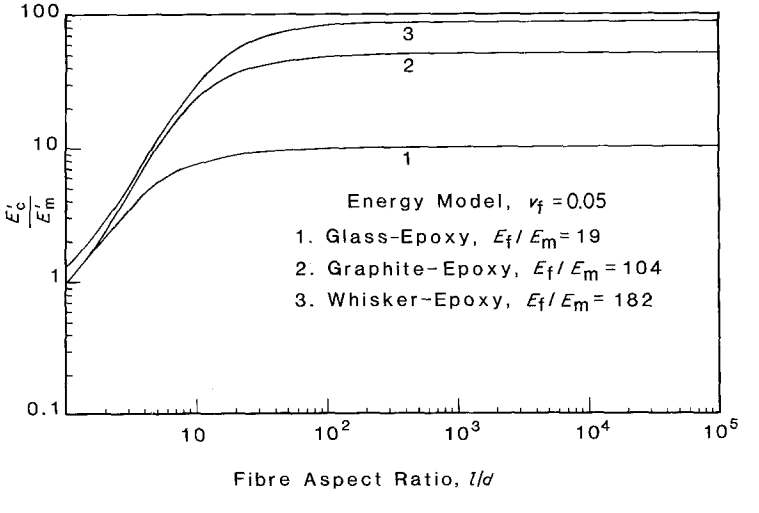

Figure 8 Effect of fibre stiffness on storage modulus of discontinuous aligned composites.

2, 11, 12, 14 and A2 may be expressed in terms of the fibre volume fraction, v_f, for a specified packing array. For example,

$$\left(\frac{R}{r_0}\right)^2 = \frac{\pi}{2\sqrt{3}v_f} \text{ for a hexagonal array,} \tag{A3}$$

and

$$\left(\frac{R}{r_0}\right)^2 = \frac{\pi}{4v_f} \text{ for a square array.} \tag{A4}$$

In all the analytical results presented in Figs 3 to 8, a hexagonal array has been assumed. Substituting these expressions in Equation 2, we find that

$$\frac{\beta l}{2} = K_1 \frac{l}{d}\left[\frac{G'_m}{E'_f}\right]^{1/2}, \tag{A5}$$

where

$$K_1 = \left[\frac{2}{\ln(1/cv_f^{1/2})}\right]^{1/2}$$

$$d = 2r_0,$$

and

$$c^2 = \begin{cases} 2\sqrt{3}/\pi & \text{for a hexagonal array} \\ 4/\pi & \text{for a square array.} \end{cases}$$

Therefore

$$\frac{\beta^* l}{2} = K_1 \frac{l}{d}\left[\frac{G'_m(1+i\eta_{Gm})}{E'_f(1+i\eta_f)}\right]^{1/2}. \tag{A6}$$

Since the loss factors are very small, higher order terms like η_f^2 and $\eta_{Gm}\eta_f$ can be neglected and Equation A6 simplified to

$$\frac{\beta^* l}{2} = \frac{\beta l}{2}[1 + \tfrac{1}{2}i(\eta_{Gm} - \eta_f)]. \tag{A7}$$

Similarly, using a Taylor's series approximation and neglecting higher order terms in the loss factors, we get

$$\tanh\frac{\beta^* l}{2} = \tanh\frac{\beta l}{2} + \frac{i}{2}\frac{\beta l}{2}\cdot\frac{(\eta_{Gm} - \eta_f)}{\cosh^2 \beta l/2}. \tag{A8}$$

Equation A8 was used to obtain Equations 21 and 22.

Finally, the factor K in Equation 31 can be found from Equation A5 as

$$K = \left(\frac{E'_f}{G'_m}\right)^{1/2} \frac{[\ln(1/cv_f^{1/2})]^{1/2}}{2\sqrt{2}}. \tag{A9}$$

References

1. C. W. BERT and R. R. CLARY, in "Composite Materials: Testing and Design (3rd Conference)" ASTM STP 546 (The American Society for Testing and Materials, Philadelphia, 1974) pp. 250–265.
2. R. F. GIBSON and R. PLUNKETT, *Shock and Vibration Digest* 9 (2) (1977) 9.
3. R. F. GIBSON and D. G. WILSON, *ibid.* **11** (10) (1979) 3.
4. C. W. BERT, in "Damping Applications for Vibrations Control", ASME AMD-38 (The American Society of Mechanical Engineers, New York, 1980) pp. 53–63.
5. D. MCLEAN and B. E. READ, *J. Mater. Sci.* **10** (1975) 481.
6. R. F. GIBSON and A. YAU, *J. Comp. Mater.* **14** (1980) 155.
7. R. PLUNKETT and C. T. LEE, *J. Acoust. Soc. Amer.* **48** (1970) 150.
8. H. L. COX, *Brit. J. Appl. Phys.* **3** (1952) 72.
9. N. F. DOW, "Study of Stresses Near a Discontinuity in a Filament-Reinforced Composite Metal", General Electric Space Sciences Laboratory Report No. R63SD61 (1963).
10. B. W. ROSEN, "Fibre Composite Materials" (American Society of Metals, Metals Park, Ohio, 1964) ch. 3.
11. A. KELLY and W. R. TYSON, in "High Strength Materials", edited by V. F. Zackay (Wiley, New York, 1965) ch. 13.
12. G. E. SMITH and A. J. M. SPENCER, *J. Mech. Phys. Solids* **18** (1970) 81.
13. W. R. TYSON and G. J. DAVIES, *Brit. J. Appl. Phys.* **16** (1965) 199.
14. A. S. CARRARA and F. J. MCGARRY, *J. Comp. Mater.* **2** (1968) 222.
15. T. F. MACLAUGHLIN, *ibid* **2** (1968) 44.
16. M. J. IREMONGER and W. G. WOOD, *J. Strain Anal.* **4** (1969) 121.
17. RICHARD M. BARKER and THOMAS F. MACLAUGHLIN, *J. Comp. Mater.* **5** (1971) 492.
18. Z. HASHIN, *Int. J. Solid Struct.* **6** (1970) 539.
19. R. F. GIBSON, A. YAU and D. A. RIEGNER, *Exp. Techniques* **6** (1982) 10.
20. R. F. GIBSON and R. PLUNKETT, *J. Comp. Mater.* **10** (1976) 325.
21. "Vibration Damping of Composites Reinforced with Kevlar 49 Aramid, Graphite and Fiberglass", E. I. duPont de Nemours & Co Textile Fibers Department Memo No. 19, June (1980).
22. J. V. MILEWSKI, Whiskers and Microfibers, in "Additives for Plastics", Vol. 1 (Academic Press, New York, 1978).
23. C. T. CHON and C. T. SUN, *J. Mater. Sci.* **15** (1980) 931.
24. S. V. KULKARNI, C. H. ZWEBEN and R. B. PIPES, (eds.) "Composite Materials in the Automotive Industry" (ASME, New York, 1978).

Received 16 April
and accepted 8 May 1982